

NASA satellite measurements show global-scale reductions in free tropospheric ozone in 2020 and again in 2021 during COVID-19

Jerry R. Ziemke^{1,2}, Natalya A. Kramarova¹, Stacey M. Frith^{1,3}, Liang-Kang Huang^{1,3}, David P. Haffner^{1,3}, Krzysztof Wargan^{1,3}, Lok N. Lamsal^{1,4}, Gordon J. Labow^{1,3}, Richard D. McPeters¹, Pawan K. Bhartia^{1,5}

¹ NASA Goddard Space Flight Center, Greenbelt, Maryland, USA

² Goddard Earth Sciences Technology and Research (GESTAR) / Morgan State University, Baltimore, Maryland, USA

³ Science Systems and Applications Inc. (SSAI), Lanham, Maryland, USA

⁴ University of Maryland Baltimore County, Baltimore, Maryland, USA

⁵ Emeritus, NASA Goddard Space Flight Center, Greenbelt, Maryland, USA

Abstract

NASA satellite measurements show that ozone reductions throughout the Northern Hemisphere (NH) free troposphere reported for spring-summer 2020 during the CoronaVirus Disease 2019 (COVID-19) pandemic have occurred again in spring-summer 2021. The satellite measurements show that tropospheric column ozone (TCO) (mostly representative of the free troposphere) for 20°N-60°N during spring-summer for both 2020 and 2021 averaged ~3 Dobson Units (DU) (or ~7-8%) below normal. These ozone reductions in 2020 and 2021 were the lowest in the 2005-2021 record. We also include satellite measurements of tropospheric NO₂ that exhibit reductions of ~10-20% in the NH in early spring-to-summer 2020 and 2021, suggesting that reduced pollution was the main cause for the low anomalies in NH TCO in 2020 and 2021. Reductions of TCO ~2 DU (7 %) are also measured in the Southern Hemisphere in austral summer but are not associated with reduced NO₂.

Plain Language Summary

30 The decreases in ozone throughout the NH free troposphere in spring-summer 2020 as reported
31 by several previous studies are shown from satellite measurements to have repeated in spring-
32 summer 2021 with similar extent. The satellite data indicate decreases in tropospheric column
33 ozone (indicative mostly of free tropospheric ozone) of ~5-10% throughout the NH in spring-
34 summer months for both 2020 and 2021. These ozone reductions in 2020 and 2021 were the
35 lowest on record for the 2005-2021 time period considered in this study. The satellite data also
36 exhibit smaller decreases in the SH of ~7% in austral summer (December 2020-February 2021).
37 The anomalous reductions in tropospheric ozone in the NH are shown to be directly correlated
38 with reductions in anthropogenic pollution-related NO₂ during spring-summer 2020 and 2021,
39 but not in the SH in summer. We conclude from our analyses that decreases in pollutants due to
40 reduced human activities including lockdowns during COVID-19 likely led to most of the
41 decreases measured in free tropospheric ozone throughout the NH in spring-summer 2020 and
42 2021.

43

44 **1. Introduction.**

45

46 In early 2020, soon after the beginning of the global COVID-19 pandemic, extensive
47 international efforts were taken in attempt to reduce the spread of the virus. These efforts
48 included lockdowns and reduced activities of many private and public businesses, schools, and
49 travel. A result was unprecedented decreases in Northern Hemisphere (NH) pollution including
50 important ozone precursors nitrogen oxides (NO_x = nitric oxide (NO) + nitrogen dioxide (NO₂))
51 and Volatile Organic Compounds (VOCs). The decreases in pollution and subsequent changes
52 in tropospheric ozone, particularly in the NH, has led to a large number of published articles on
53 this subject (e.g., Liu et al., 2020; Bauwens et al., 2020; Sicard et al., 2020; Bray et al., 2021;
54 Campbell et al., 2021; Keller et al., 2021; Bouarar et al., 2021; Steinbrecht et al., 2021;
55 Elshorbany et al., 2021; Stavrou et al. 2021; Miyazaki et al., 2021; Jensen et al., 2021;
56 Pakkattil et al., 2021). These studies have shown numerous cases of large reductions in NO₂,
57 VOCs, and other pollutants in the troposphere including free-tropospheric ozone during spring-
58 summer 2020 that reached 5-10% deficits or greater throughout the NH, particularly in urban
59 environments.

60

61 Although studies have measured ozone reductions throughout the NH free troposphere in spring-
62 summer 2020, ozone in the boundary layer (BL) during these months has been shown to have
63 instead largely increased in and around urban areas (e.g., Sicard et al., 2020; Yin et al, 2021, Liu
64 et al., 2021, and references therein). These studies suggest that the increases in surface ozone
65 could be due to a weakening of a titration effect on ozone in accordance with 2020
66 meteorological conditions and relative levels of NO_x versus VOC reductions. Campbell et al.
67 (2021) and Parker et al. (2022) also show increases up to about +40% for near-surface ozone
68 concentrations in spring-summer 2020 over the US in urban environments. Campbell et al.
69 (2021) further describe the complex nature of the BL chemistry (NO_x limited versus VOC
70 limited) whereby the widespread emission decreases in the US in 2020 in a general sense led to
71 increases of BL ozone in urban areas, but widespread decreases in rural regions.

72
73 Based on satellite observations from the TROPOspheric Monitoring Instrument (TROPOMI) and
74 Infrared Atmospheric Sounding Interferometer (IASI) instrument and a model simulation,
75 Stavrakou et al. (2021) identified pollutant reductions in early 2020 over China including
76 peroxyacyl nitrates (PAN) by 21%, NO₂ by 15-40%, and glyoxal (CHOCHO) by 3%. Bauwens
77 et al. (2020), using TROPOMI and the Ozone Monitoring Instrument (OMI) satellite
78 measurements, identified large drops in NO₂ in early 2020 varying from 20% to 40% relative to
79 the pre-COVID-19 time period over the US, western Europe, South Korea and China. Jensen et
80 al. (2021) identified pollution reductions of 40-60% for industry and about 70% for traffic over
81 China in early 2020 using TROPOMI and ground-based measurements. Miyazaki et al. (2021),
82 using a chemical data assimilation system, identified drops of 15% in global NO_x with up to 25%
83 regional drops in NO_x for April-May 2020. For VOCs, studies also report large reductions in the
84 NH in 2020. For example, Jensen et al. (2021) found 40-70% anthropogenic reductions in VOCs
85 in early spring 2020 in Changzhou, China. Pakkattil et al. (2021) used ground measurements to
86 show drops in VOCs in early spring 2020 over major metropolitan cities in India, with up to 82%
87 reductions in the first phase of spring-time lockdown compared to pre-lockdown.

88
89 For tropospheric ozone, studies show anomalous reductions during spring-summer 2020
90 throughout the NH free troposphere. Steinbrecht et al. (2021) identified a 7% reduction of ozone
91 throughout the NH free troposphere during spring-summer 2020 from analysis of ozonesondes,

92 lidar, and a model; they attributed the loss mostly to reductions in ozone precursors, with
93 possibly up to 1/4 of the reductions coming from the record low Arctic stratospheric ozone in
94 winter-spring 2020 injected into the troposphere. Bouarar et al. (2021) used a model simulation
95 to indicate 5-15% reductions of NH zonally averaged ozone in the free troposphere in winter-
96 spring 2020; they attributed about 1/3 coming from reduction of air traffic, 1/3 from reduction in
97 surface emissions, and 1/3 from meteorological conditions that includes the 2020 Arctic
98 stratospheric ozone depletion. Using satellite data from the Earth Polychromatic Imaging
99 Camera (EPIC) instrument, Kramarova et al. (2021) showed anomalous decreases in zonal-mean
100 tropospheric column ozone throughout the NH extra-tropics of about 2-4 DU (5-10%) in spring-
101 summer 2020. Elshorbany et al. (2021) also described reductions of several percent in
102 tropospheric ozone over the continental US using the Ozone Mapping and Profiler Suite (OMPS)
103 satellite data.

104

105 There are currently few articles on COVID-related global pollution for year 2021 relative to
106 2020 and previous years. The general consensus is that global pollution was greater in 2021
107 compared to 2020, but still lower than in years prior to COVID-19. Saharan et al. (2022) shows
108 higher measured surface pollutants in 2021 in Delhi, India compared to 2020, but still less than
109 pre-COVID; their Table 2 for both March and April shows reductions in CO, O₃, and NO_x
110 during 2021 relative to years 2018 and 2019. Sarmadi et al. (2021) evaluated 87 world city sites
111 in both the NH and SH and state that air quality indices measured for CO, NO₂, and particulate
112 matter (PM) with sizes less than 2.5 μm and 10 μm (PM_{2.5} and PM₁₀) were overall lower in 2020
113 by 7.4-20.5 % and higher in 2021 by 4.3-7.5 % when compared to 2019; however, their Fig. 3
114 indicates that PM_{2.5} and PM₁₀ for year 2021 still remained low on average for at least 25 city
115 sites (mostly in the NH) when compared to years 2018 and 2019. The International Civil
116 Aviation Organization (ICAO, 2022) shows that world air traffic increased in year 2021 relative
117 to 2020 but remained about 49% below the 2019 level. As comparison, the US Bureau of
118 Transportation Statistics for July 2021 ([https://www.bts.gov/newsroom/july-2021-us-airline-
119 traffic-data-0](https://www.bts.gov/newsroom/july-2021-us-airline-traffic-data-0)) indicates US passenger air travel (domestic + international) was up 207% from
120 July 2020; however, air travel was still down in July 2021 by 15.5% compared to July 2019,
121 before the pandemic.

122

123 This paper provides a global evaluation of reductions in free tropospheric ozone in years 2020
124 and 2021 during the COVID-19 pandemic using ozone measurements from combined EPIC,
125 OMPS, OMI, and Microwave Limb Sounder (MLS) satellite instruments. A primary motivation
126 is to show that there were large planetary-scale decreases of NH tropospheric ozone in year 2021
127 that were similar to the decreases in year 2020. Our study also includes satellite observations of
128 NO₂ and aerosols and offers plausible explanations for the tropospheric ozone reductions.
129 Section 2 discusses the tropospheric ozone measurements, section 3 describes results, and section
130 4 summarizes our findings.

131

132 **2. Tropospheric Ozone Measurements.**

133

134 For deriving tropospheric column ozone (TCO), we use measurements of total column ozone
135 from three separate satellite instruments for January 2015 – August 2021 when all three
136 measurements overlapped. These three satellite instruments are the Deep Space Climate
137 ObserVatoRy (DSCOVR) EPIC (Herman et al., 2018), the Aura OMI (Levelt et al., 2006), and
138 the Suomi National Polar Partnership (SNPP) OMPS nadir mapper (McPeters et al., 2019). TCO
139 for all three datasets is determined by subtracting stratospheric column ozone (SCO) from total
140 column ozone, where SCO is derived by vertically integrating Global Modeling and Assimilation
141 Office (GMAO) Modern-Era Retrospective analysis for Research and Applications-2 (MERRA-
142 2) assimilated Aura MLS ozone profiles (Wargan et al., 2017; Gelaro et al., 2017) from the top
143 of the atmosphere down to the tropopause. The tropopause pressure is taken from MERRA-2
144 analyses (GMAO, 2015) using the standard potential vorticity – potential temperature (PV- θ)
145 definition (i.e., 2.5 PV units, 380 K). The SCO synoptic fields from MERRA-2 at 3-hour
146 intervals are space-time co-located on a pixel-by-pixel basis via temporal interpolation for each
147 of the three satellites total ozone measurement footprints independently. All TCO datasets
148 represent daily global maps (outside polar night regions) at 1° latitude × 1° longitude gridding.
149 Details regarding individual TCO measurements for EPIC, OMPS, and OMI with MERRA-2
150 SCO are discussed by Kramarova et al. (2021) and Elshorbany et al. (2021). The sensitivity of
151 detecting tropospheric ozone for EPIC, OMI, and OMPS is ~100% above 5 km altitude but
152 decreases to ~40-50% for ozone columns below 5 km; TCO measured from the three instruments
153 therefore represents mostly free tropospheric ozone. Uncertainties (1σ precision values) in

154 gridded TCO were determined by 1-1 comparisons with daily ozonesondes, indicating zero to ± 4
155 DU offsets and standard deviations of 2-7 DU (smallest in tropics) for EPIC, OMI, and OMPS
156 TCO measurements; precision for monthly-mean gridded TCO for each product varies ~ 0.5 -1.5
157 DU.

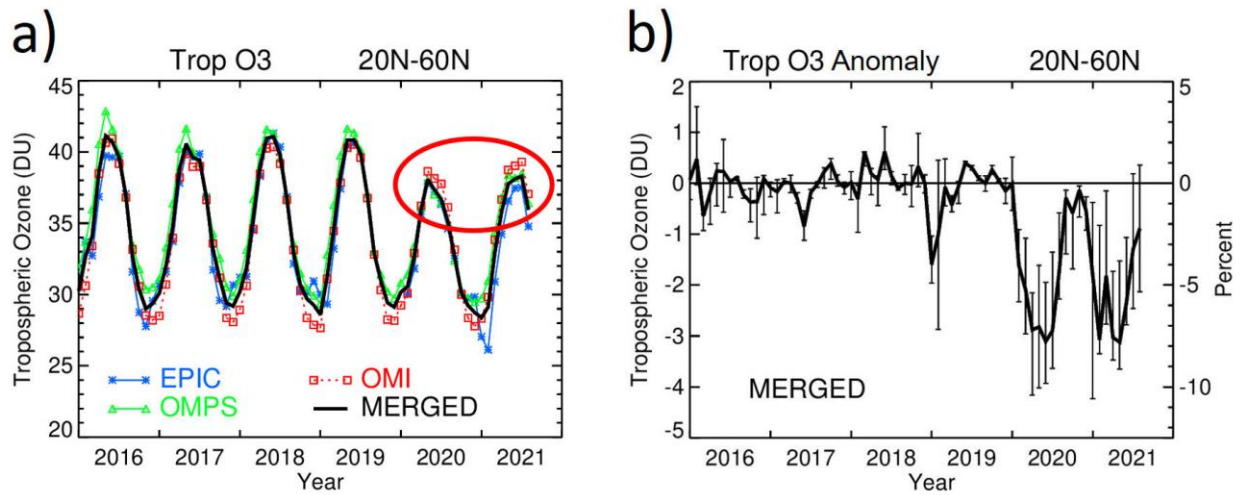
158
159 We derive a “merged” TCO dataset by statistically averaging the TCO daily measurements from
160 the three satellite measurements based on the extent of their daily global coverage. This was
161 done by weighting OMPS and EPIC ozone by ~ 1.0 and OMI by ~ 0.7 because 30% of OMI
162 measurements are missing due to the OMI row anomaly. The reason for generating the merged
163 data is to produce the best overall dataset for studying inter-annual changes in TCO. Inter-
164 annual anomalies of TCO were determined relative to a 12-month baseline average TCO field for
165 2016-2019 (as a function of longitude, latitude, and month). Year 2015 was not included in the
166 baseline TCO calculation due to 2015-2016 being an extreme El Nino event greatly affecting
167 TCO for September-November 2015; also, the EPIC measurements begin June 2015 and are
168 sparse until August 2015. In addition, we analyzed an 18-year extended record of merged TCO
169 by appending the 2015-2021 record with OMI/MLS TCO measurements (Ziemke et al., 2006)
170 for October 2004 – December 2014 to evaluate the long-term significance of observed reductions
171 in 2020-2021. Figures and discussion regarding merged TCO and the individual satellite
172 measurements of TCO from EPIC, OMI, and OMPS are provided in the Supporting Information.

173 174 **3. Results.**

175 **3.1. Reduction of Zonal Mean Tropospheric Ozone in the NH for both 2020 and 2021.**

176
177 The satellite data show that the reductions of 5-10% in free tropospheric ozone throughout the
178 NH in spring-summer 2020, as reported by many studies, has occurred again in spring-summer
179 2021 (Fig. 1). Figure 1a shows TCO monthly time series averaged over the NH for latitudes
180 20°N - 60°N for the three satellite records along with the merged dataset. The seasonal cycle in
181 tropospheric ozone is very pronounced in the NH with the seasonal peak in spring-summer
182 months driven by combined effects of spring-summer stratosphere-troposphere exchange (STE)
183 and ozone precursors from natural and anthropogenic sources (Lelieveld and Dentener, 2000; de
184 Laat et al., 2005, and references therein). The large red oval in Figure 1a highlights a ~ 3 DU

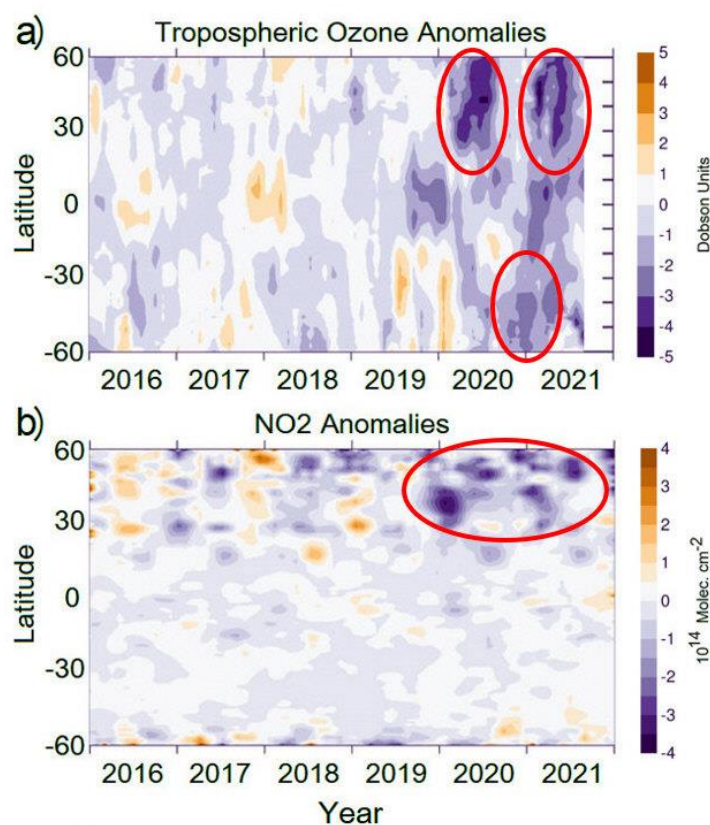
185 decrease in NH TCO during spring-summer 2020 that was repeated nearly identically in spring-
 186 summer 2021. The anomalous decreases in TCO in 2020 and 2021 are illustrated more clearly in
 187 Figure 1b which plots inter-annual anomaly time series of merged TCO with respect to 2016-
 188 2019 seasonal averages. The right vertical axis in Figure 1b shows that drops of 3 DU of TCO in
 189 spring-summer months in both 2020 and 2021 correspond to percentage decreases of ~7-8%.
 190 These percent decreases are similar to the 7% decreases in free tropospheric ozone throughout
 191 the NH in year 2020 reported by Steinbrecht et al. (2021) from ozonesonde data. The 18-year
 192 merged TCO record (Supporting Information, Fig. S7) indicates that the decreases in NH TCO
 193 during spring-summer 2020 and 2021 were larger than in any previous year extending back to
 194 year 2005.



195
 196 **Figure 1.** (a) Monthly time series of TCO (in DU) averaged over the NH for 20°N-60°N for the
 197 three instrument measurements along with the combined EPIC+OMPS+OMI merged time series
 198 (indicated). Red oval highlights anomalous drops of ~3 DU in spring-summer of both 2020 and
 199 2021. (b) Inter-annual anomaly time series of merged monthly TCO (in DU) for 2016-2021
 200 relative to the baseline TCO (see text). Vertical bars show absolute maximum and absolute
 201 minimum TCO inter-annual anomalies for the three instruments during each month about the
 202 merged mean value.

203
 204 We have compared the anomalous drops in TCO in years 2020-2021 with changes in
 205 tropospheric NO₂ (Fig. 2) and aerosol measurements to evaluate possible links to pollution
 206 including anthropogenic emissions, smoke from biomass burning and wildfires, and Saharan

207 dust. (Supporting Information, Fig. S11). In Fig. 2a the three red ovals highlight anomalous
 208 decreases in TCO in the NH during spring-summer 2020 and 2021 (~3-5 DU in both years) and
 209 in the SH (~2 DU) during summertime (December 2020 – February 2021). These drops in TCO
 210 are larger than the 1σ average inter-annual variability of ~1 DU (Supporting Information, Fig.
 211 S9). In the tropics, decreases in TCO in 2019 are related to a strong positive phase of the Indian
 212 Ocean Dipole (IOD) which reduced TCO over tropical Africa and east of Africa due an increase
 213 in deep convection east of Africa that lofted low ozone air from the oceanic BL into the free
 214 troposphere (Ratna et al., 2021; Supporting Information, Fig. S10). A close inspection of Fig. 2a
 215 indicates that TCO reductions in mid-latitudes were stronger by ~1 DU in 2020 compared to
 216 2021.
 217



218
 219 **Figure 2.** (a) Monthly zonal-mean inter-annual anomalies of merged TCO (in DU) for 60°S-
 220 60°N and period January 2016-August 2021. Inter-annual changes were derived by subtracting
 221 2016-2019 average seasonal cycles from the data. Red ovals designate months and latitudes
 222 where greatest anomalous reductions in extra-tropical TCO in 2020 and 2021 occurred. (b)

223 Similar to (a) but for OMI NO₂ tropospheric columns in units of 10¹⁴ molec. cm⁻². Red oval
224 highlights anomalous drops in early spring to summer months of both 2020 and 2021 in the NH
225 extra-tropics.

226
227 Figure 2b shows corresponding changes in OMI NO₂ (version 4.0, Lamsal et al., 2021). Similar
228 to TCO, largest decreases for NO₂ of -2.0×10^{14} to -4.0×10^{14} molec. cm⁻² occur in early spring
229 into summer for years 2020 and 2021 in the NH extra-tropics (large red oval). In the SH there
230 are no obvious NO₂ anomalies for any year. Estimated 1 σ uncertainty for NO₂ monthly means is
231 about 0.5×10^{13} molec. cm⁻² (e.g., Marchenko et al., 2015; Supporting Information, Fig. S3). The
232 space-time patterns for NH TCO and NO₂ during spring-summer 2020-2021 in Fig. 2 generally
233 coincide, but not precisely, perhaps due to effects of titration, chemical lifetimes, and
234 meteorological effects. Similar to TCO, reductions of NO₂ columns in year 2021 in NH mid-
235 latitudes are also smaller than in year 2020 by about 1×10^{14} to 2×10^{14} molec. cm⁻².

236
237 Wildfires can generate several tropospheric ozone precursors including NO_x, CH₄, VOCs, and
238 CO. We analyzed anomalies in OMPS Aerosol Index (AI) (Torres et al., 2018), shown in Fig.
239 S11 of the Supporting Information. Positive anomalies in AI indicate the presence of absorbing
240 aerosols such as smoke and dust. The NH wildfires in both years 2020 and 2021 caused positive
241 anomalies in AI with the peak extent in August-September, coinciding with the disappearance of
242 TCO negative anomalies (Supporting Information, Fig. S11); this suggests that smoke from
243 wildfires may have aided the return of tropospheric ozone toward normal late summer/autumn
244 amounts in both 2020 and 2021. Meteorological conditions that control the strength of STE were
245 anomalous in NH in spring 2020 (e.g. Lawrence et al., 2020), but 2021 conditions were close to
246 climatological means, suggesting STE is not driving the anomalies. Therefore, we conclude
247 from Fig. 2 that it is plausible that decreases in TCO in the NH in spring-summer of 2020 and
248 2021 are attributed largely to decreases in emissions (e.g., NO₂ in both years) and reduced
249 photochemical production of ozone in the troposphere, although wildfires may have mitigated
250 the impact in late summer and autumn.

251
252 We did not find any clear connection in the SH between TCO decreases and negative anomalies
253 in either NO₂ or smoke aerosols (Supporting Information, Fig. S11). The decreases of TCO in

254 the SH in 2020-2021 may have been related to anomalies in STE in the presence of a strong and
255 long-lasting Antarctic polar vortex in the SH in October-December 2020 that resulted in
256 substantial stratospheric ozone loss (Stone et al., 2021; Kramarova et al., 2021); however,
257 establishing such a connection requires modeling and is beyond the scope of our study.

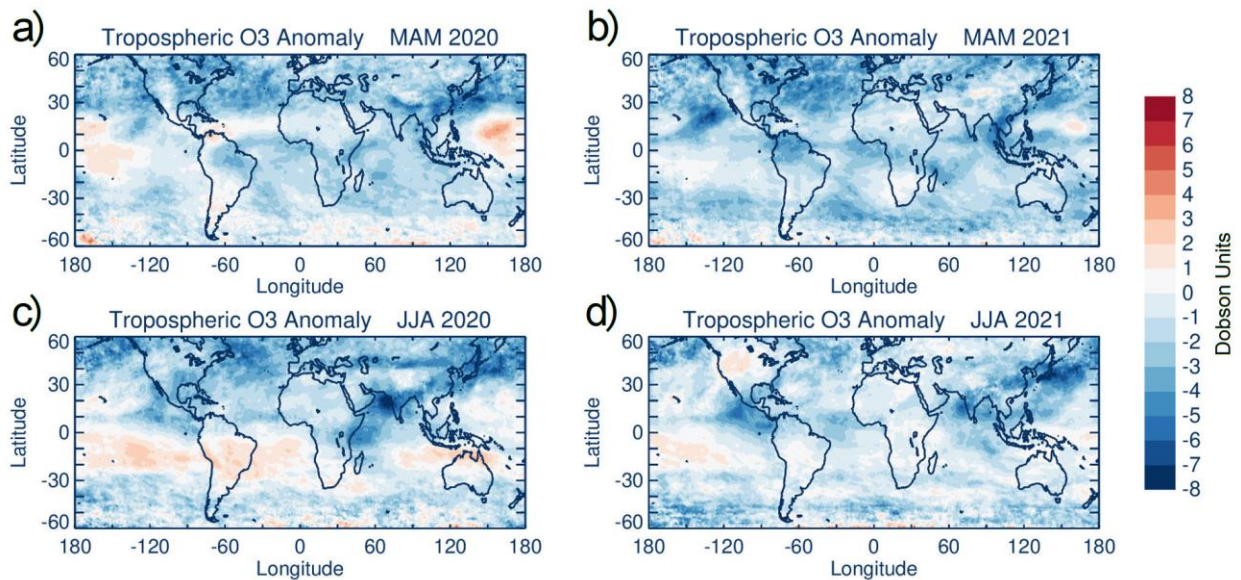
258

259 3.2. Global Patterns of Tropospheric Ozone in Spring-Summer 2020 and 2021.

260

261 Figure 3 shows spatial distributions of inter-annual TCO anomalies averaged separately for NH
262 spring (Fig. 3a and 3b) and NH summer (Fig. 3c and 3d) of 2020 and 2021. Decreases in TCO
263 for both spring and summer 2020 (Fig. 3a and 3c) occur over the entire NH as was noted earlier
264 for Fig. 2a. The NH TCO negative anomaly patterns are similar in spring 2020 and 2021 with
265 variations of -1 DU to -5 DU (Figs. 3a and 3b), however the TCO decreases in summer 2021
266 (Fig. 3d) are smaller than in summer 2020 (Fig. 3c) by ~2 DU throughout the NH mid-high
267 latitudes (Supporting Information, Fig. S12), Positive changes in TCO up to +2 DU (shaded
268 orange) in the SH occurred in summer 2020; these positive TCO anomalies coincide with
269 increases in NO₂ over S. America and Africa in this same latitude band (Supporting Information,
270 Fig S3c), suggesting an increase in production and long-range transport of tropospheric ozone.

271



272

273 **Figure 3.** Year 2020 TCO inter-annual anomalies (see text) for (a) March-April-May (MAM)

274 spring season and (c) June-July-August (JJA) summer season. (b) and (d) are the same as (a) and

275 (c), respectively, but for year 2021. All TCO (in DU) is derived from merged data with
276 anomalies based on removing 2016-2019 average seasonal cycles.

277
278 In summer 2021, negative TCO anomalies (Fig. 3d) are mostly observed over Asia, and TCO
279 changes are positive over some parts of the Asian continent and over the western-central US
280 (shaded orange). The TCO increases over the US of ~1-2 DU (Fig. 3d) coincide with similar
281 increases in NO₂ over the US in summer 2021 (Supporting Information, Fig. S3d). The intense
282 wildfires over California in July-September 2021 (Supporting Information, Fig. S11) could have
283 contributed to the positive TCO anomalies over the US in summer 2021.

284

285 **4. Summary and Discussion.**

286

287 Combined satellite measurements from EPIC, OMPS, OMI, and MLS instruments show that the
288 anomalous reductions in free tropospheric ozone throughout the NH reported for spring-summer
289 2020 have occurred again in spring-summer 2021. Due to limited sensitivity for detecting BL
290 ozone variability (~40-50%), the satellite-derived TCO largely represents ozone in the free
291 troposphere. Satellite measurements of OMI NO₂ and OMPS aerosol index were also included
292 to evaluate the role of pollution from anthropogenic emissions and wildfires on observed
293 changes in TCO.

294

295 Reductions in NH TCO during spring 2021 were similar to spring 2020; however, reductions in
296 NH TCO in summer 2021 were not as large and uniformly spread as in summer 2020. There
297 were in fact regions of positive TCO anomalies in summer 2021, especially over the US which
298 coincided with regional increases in OMI NO₂ and intense wildfires. Most of the decreases in
299 NH TCO in spring-summer 2020 and 2021 occurred over ocean, downwind of continental
300 pollution sources, indicating effects of long-range transport. Average decreases in 20°N-60°N
301 TCO in spring-summer 2020 and 2021 were ~3 DU (~7-8%) relative to 2016-2019 average
302 ozone levels, which were larger than the typical 1-1.5 DU inter-annual variabilities seen in the
303 previous years since 2005 (Supporting Information, Fig. S9). Regional reductions in NH TCO
304 measured for 2020 and 2021 varied up to ~3-5 DU (~7-13%).

305

306 Anomalous reductions in TCO of about 2 DU (~7%) were measured in the SH centered around
307 austral summer (December 2020 – February 2021). These decreases did not coincide with
308 similar decreases in OMI tropospheric NO₂. Other factors such as an unusually large and long-
309 lasting Antarctic ozone hole during September-December 2020 and subsequent stratospheric
310 injection of anomalously low ozone air into the troposphere might be responsible for the low
311 anomalies in SH TCO. A quantitative evaluation of SH TCO anomalies would require a
312 modeling simulation which is beyond the scope of this study.

313

314 We also analyzed a merged 18-year extended record (October 2004 – December 2021) of TCO
315 to evaluate the significance of the reductions in TCO in 2020 and 2021 in relation to previous
316 years (Supporting Information, Figs. S6 and S7). We found that the decreases in TCO in the NH
317 averaged over 20°N-60°N during spring-summer 2020 and 2021 were greater than for any
318 previous year since 2005 despite the presence of a decadal positive trend in NH tropospheric
319 ozone averaging ~1.5 DU decade⁻¹ (Supporting Information, Fig. S7).

320

321 There are several important implications for these results. The 2014 Inter-governmental Panel
322 on Climate Change (IPCC) report lists tropospheric ozone as the third most influential
323 greenhouse gas following methane and carbon dioxide, with tropospheric ozone contributing on
324 average to net warming of the atmosphere by about +0.4 W m⁻². The reductions in TCO
325 throughout the NH in spring-summer 2020 and 2021 of ~7-8% on average (and up to 7-13%
326 regionally) have therefore had a proportionately sizable effect in reducing atmospheric warming
327 and an opposite offsetting effect on the increases in warming due to positive trends in
328 tropospheric ozone over the last two decades. The amplitude of the seasonal cycle in NH TCO
329 was reduced by about 15% in 2020 and 2021 (i.e., about 3 DU out of 20 DU) relative to previous
330 years. These changes will have an impact on calculations of long-term seasonal trends in
331 tropospheric ozone. The reduction in TCO in 2020 and 2021 provide a valuable reference for
332 evaluating model simulations that use reported emission inventories to simulate changes in
333 tropospheric ozone and other trace gas concentrations.

334

335 **Acknowledgements.** We thank the NASA Jet Propulsion Laboratory MLS team for the MLS
336 v4.2 ozone dataset, and the EPIC, OMPS, and OMI ozone processing teams. MERRA-2 is an

337 official product of the Global Modeling and Assimilation Office at NASA GSFC. We also thank
338 the NASA Center for Climate Simulation (NCCS) for providing high-performance computing
339 resources.

340
341 **Data availability.** The data description for MLS v4.2 ozone and links to the data can be obtained
342 from the following websites: <https://mls.jpl.nasa.gov/> (NASA MLS division, 2022) and
343 <https://disc.gsfc.nasa.gov/> (NASA MLS science research group, 2022). The MERRA-2 GMI
344 model description and access are available from [https://acd-
345 ext.gsfc.nasa.gov/Projects/GEOSCCM/MERRA2GMI/](https://acd-ext.gsfc.nasa.gov/Projects/GEOSCCM/MERRA2GMI/) (Code 614 GMI modeling group, 2022).
346 EPIC tropospheric ozone data are available from the Langley ASDC data portal
347 (<https://asdc.larc.nasa.gov/>). Tropospheric ozone data for OMI and OMPS are available from the
348 NASA GSFC Code 614 webpage https://acd-ext.gsfc.nasa.gov/Data_services/cloud_slice/.

349
350 **Financial support.** This research has been supported by the NASA programmatic fund “Long-
351 term ozone trends” (project no. WBS 479717). Jerald R. Ziemke and Natalya A. Kramarova
352 were also supported by the NASA ROSES proposal “Improving total and tropospheric ozone
353 column products from EPIC on DSCOVR for studying regional scale ozone transport” (grant no.
354 18-DSCOVR18-0011, DSCOVR Science Team). Gordon J. Labow, Stacey M. Frith, David P.
355 Haffner and K. Wargan were supported under NASA contract NNG17HP01C.

356 357 **References**

358
359 Bauwens, M., S. T. Compernelle, J.-F. Müller, J. van Gent, H. Eskes, P. F. Levelt, R. van der A,
360 J. P. Veefkind, J. Vlietinck, H. Yu, C. Zehner (2020). Impact of coronavirus outbreak on NO₂
361 pollution assessed using TROPOMI and OMI observations, *Geophys. Res. Lett.*, 47,
362 e2020GL087978, <https://doi.org/10.1029/2020GL087978>.

363
364 Bray, C. D., A. Nahas, W.H. Battye, V.P. Aneja Impact of lockdown during the COVID-19
365 outbreak on multi-scale air quality *Atmos. Environ.* (2021),
366 <https://doi.org/10.1016/j.atmosenv.2021.118386>.

367

368 Bouarar, I., Gaubert, B., Brasseur, G. P., Steinbrecht, W., Doumbia, T., Tilmes, S., et al. (2021).
369 Ozone anomalies in the free troposphere during the COVID-19 pandemic. *Geophys. Res. Lett.*,
370 48, e2021GL094204. <https://doi.org/10.1029/2021GL094204>.
371

372 Campbell, P. C., D. Tong, Y. Tang, B. Baker, P. Lee, R. Saylor, A. Stein, S. Ma, and L. Lamsal
373 (2021). Impacts of the COVID-19 Economic Slowdown on Ozone Pollution in the U.S.
374 *Atmospheric Environment*, <https://doi.org/10.1016/j.atmosenv.2021.118713>.
375

376 de Laat, A. T. J., I. Aben, and G. J. Roelofs (2005). A model perspective on total tropospheric
377 O₃ column variability and implications for satellite observations, *J. Geophys. Res.*, 110, D13303,
378 doi:10.1029/2004JD005264.
379

380 Elshorbany, Y. Y., H. C. Kapper, J. R. Ziemke, & S. A. Parr (2021). The status of air quality in
381 the United States during the COVID-19 pandemic: A remote sensing perspective, *Rem. Sens.*,
382 13(3), 369, <https://doi.org/10.3390/rs13030369>.
383

384 Global Modeling and Assimilation Office (GMAO) (2015), MERRA-2 tavg3_3d_asm_Nv: 3d,3-
385 Hourly,Time-Averaged,Model-Level,Assimilation,Assimilated Meteorological Fields V5.12.4,
386 Greenbelt, MD, USA, Goddard Earth Sciences Data and Information Services Center (GES
387 DISC), Accessed: September. 2021, 10.5067/SUOQESM06LPK.
388

389 Gelaro, R., W. McCarty, M.J. Suárez, R. Todling, A. Molod, L. Takacs, C.A. Randles, A.
390 Darmenov, M.G. Bosilovich, R. Reichle, K. Wargan, L. Coy, R. Cullather, C. Draper, S. Akella,
391 V. Buchard, A. Conaty, A.M. da Silva, W. Gu, G. Kim, R. Koster, R. Lucchesi, D. Merkova, J.E.
392 Nielsen, G. Partyka, S. Pawson, W. Putman, M. Rienecker, S.D. Schubert, M. Sienkiewicz, & B.
393 Zhao (2017). The Modern-Era Retrospective Analysis for Research and Applications, Version 2
394 (MERRA-2), *J. Climate*, 30, 5419–5454, <https://doi.org/10.1175/JCLI-D-16-0758.1>.
395

396 Herman, J., Huang, L., McPeters, R., Ziemke, J., Cede, A., and Blank, K. (2018). Synoptic
397 Ozone, Cloud Reflectivity, and Erythemal Irradiance from Sunrise to sunset for the Whole Earth

398 as Viewed by the DSCOVR Spacecraft from the Earth-Sun Lagrange 1 Orbit. *Atmos. Meas.*
399 *Tech.* 11, 177–194. doi:10.5194/amt-11-177-2018.

400
401 International Civil Aviation Organization (ICAO) report (2022). The impact of COVID-19 on
402 global air passenger traffic in 2021. [https://unitingaviation.com/news/economic-](https://unitingaviation.com/news/economic-development/the-impact-of-covid-19-on-global-air-passenger-traffic-in-2021/)
403 [development/the-impact-of-covid-19-on-global-air-passenger-traffic-in-2021/](https://unitingaviation.com/news/economic-development/the-impact-of-covid-19-on-global-air-passenger-traffic-in-2021/).

404
405 Inter-governmental Panel on Climate Change (IPCC) (2014). Fifth Assessment Report,
406 <https://www.ipcc.ch/>.

407
408 Jensen, A., Liu, Z., Tan, W., Dix, B., Chen, T., Koss, A., et al. (2021). Measurements of volatile
409 organic compounds during the COVID-19 lockdown in Changzhou, China. *Geophys. Res. Lett.*,
410 48, e2021GL095560, <https://doi.org/10.1029/2021GL095560>.

411
412 Keller, C. A., Evans, M. J., Knowland, K. E., Hasenkopf, C. A., Modekurty, S., Lucchesi, R. A.,
413 Oda, T., Franca, B. B., Mandarino, F. C., Díaz Suárez, M. V., Ryan, R. G., Fakes, L. H., &
414 Pawson, S (2021). Global impact of COVID-19 restrictions on the surface concentrations of
415 nitrogen dioxide and ozone, *Atmos. Chem. Phys.*, 21, 3555–3592, [https://doi.org/10.5194/acp-](https://doi.org/10.5194/acp-21-3555-2021)
416 [21-3555-2021](https://doi.org/10.5194/acp-21-3555-2021).

417
418 Kramarova N. A., J. R. Ziemke, L.-K. Huang, J. R. Herman, K. Wargan, C. J. Seftor, G. J.
419 Labow, & L. D. Oman (2021). Evaluation of Version 3 total and tropospheric ozone columns
420 from EPIC on DSCOVR for studying regional scale ozone variations. *Front. Rem. Sens.*,
421 2:734071, doi: 10.3389/frsen.2021.734071.

422
423 Kramarova, N., P. A. Newman, E. R. Nash, S. E. Strahan, C. S. Long, B. Johnson, M. Pitts, M.
424 L. Santee, I. Petropavlovskikh, L. Coy, J. de Laat, G. H. Bernhard, S. Stierle, and K. Lakkala
425 (2021). 2020 Antarctic ozone hole [in “State of the Climate in 2020”]. *Bull. Amer. Meteor. Soc.*,
426 102 (8), S345–S349, <https://doi.org/10.1175/BAMS-D-21-0081.1>.

427

428 Lamsal, L. N., Krotkov, N. A., Vasilkov, A., Marchenko, S., Qin, W., Yang, E.-S., Fasnacht, Z.,
429 Joiner, J., Choi, S., Haffner, D., Swartz, W. H., Fisher, B., & Bucsela, E. (2021). Ozone
430 Monitoring Instrument (OMI) Aura nitrogen dioxide standard product version 4.0 with improved
431 surface and cloud treatments, *Atmos. Meas. Tech.*, 14, 455–479, [https://doi.org/10.5194/amt-14-](https://doi.org/10.5194/amt-14-455-2021)
432 [455-2021](https://doi.org/10.5194/amt-14-455-2021).
433
434 Lawrence, Z. D., Perlwitz, J., Butler, A. H., Manney, G. L., Newman, P. A., Lee, S. H., & Nash,
435 E. R. (2020). The remarkably strong Arctic stratospheric polar vortex of winter 2020: Links to
436 record-breaking Arctic oscillation and ozone loss. *Journal of Geophysical Research:*
437 *Atmospheres*, **125**, e2020JD033271. <https://doi.org/10.1029/2020JD033271>.
438
439 Lelieveld, J., and F. J. Dentener (2000), What controls tropospheric ozone? *J. Geophys. Res.*,
440 105, 3531-3551, <https://doi.org/10.1029/1999JD901011>.
441
442 Levelt, P. F., H. G. H. J. van den Oord, M. R. Dobber, A. Malkki, H. Visser, J. de Vries, P.
443 Stammes, J. O. V. Lundell & H. Saari (2006). The Ozone Monitoring Instrument, *IEEE Trans.*
444 *Geophys. Rem. Sens.*, 44(5), 1093– 1101, doi: 10.1109/TGRS.2006.872333.
445
446 Liu, F., A. Page, Strode, S.A., Yoshida, Y., Choi, S., Zheng, B., Lamsal, L.N., Li, C., Krotkov,
447 N.A., Eskes, H., van der A, R., Veeffkind, P., Levelt, P.F., Hauser, O.P., & Joiner, J. (2020).
448 Abrupt decline in tropospheric nitrogen dioxide over China after the outbreak of COVID-19, *Sci.*
449 *Adv.*, 6, 28, doi:10.1126/sciadv.abc2992.
450
451 Liu, Y., T. Wang, T. Stavrakou, N. Elguindi, T. Doumbia, C. Granier, I. Bouarar, B. Gaubert, &
452 G. P. Brasseur (2021). Diverse response of surface ozone to COVID-19 lockdown in China, *Sci.*
453 *Tot. Env.*, 789, 147739, <https://doi.org/10.1016/j.scitotenv.2021.147739>.
454
455 Marchenko, S., Krotkov, N. A., Lamsal, L. N., Celarier, E. A., Swartz, W. H., and Bucsela, E. J.:
456 Revising the slant column density retrieval of nitrogen dioxide observed by the Ozone Monitor-
457 ing Instrument, *J. Geophys. Res.*, 120, 5670–5692, 2015.
458

459 McPeters, R. D., S. M. Frith, N. A. Kramarova, J. R. Ziemke, & G. J. Labow (2019). Trend
460 Quality Ozone from NPP OMPS: the Version 2 Processing, *Atmos. Meas. Tech.*, 12, 977-985,
461 <https://doi.org/10.5194/amt-12-977-2019>.
462

463 Miyazaki, K., K. Bowman, T. Sekiya, M. Takigawa, J. L. Neu, K. Sudo, G. Osterman, & H.
464 Eskes (2021). Global tropospheric ozone responses to reduced NO_x emissions linked to the
465 COVID-19 worldwide lockdowns, *Sci. Adv.*, 7, doi: 10.1126/sciadv.abf7460.
466

467 Pakkattil, A., M. Muhsin, & M. K. Ravi Varma (2021). COVID-19 lockdown: Effects on
468 selected volatile organic compound (VOC) emissions over the major Indian metro cities, *Urban*
469 *Clim.*, 37, doi: 10.1016/j.uclim.2021.100838.
470

471 Parker, L. K.; Johnson, J.; Grant, J.; Vennam, P.; Parikh, R.; Chien, C.-J.; Morris, R. Ozone
472 Trends and the Ability of Models to Reproduce the 2020 Ozone Concentrations in the South
473 Coast Air Basin in Southern California under the COVID-19 Restrictions. *Atmosphere* (2022).
474 13, 528, <https://doi.org/10.3390/atmos13040528>.
475

476 Ratna, S. B., Cherchi, A., Osborn, T. J., Joshi, M., & Uppara, U. (2021). The extreme positive
477 Indian Ocean dipole of 2019 and associated Indian summer monsoon rainfall response. *Geophys.*
478 *Res. Lett.*, 48, e2020GL091497. <https://doi.org/10.1029/2020GL091497>
479

480 Sarmadi, M., S. Rahimi, M. Rezaei, D. Sanaei, & M. Dianatinasab (2021). Air quality index
481 variation before and after the onset of COVID-19 pandemic: a comprehensive study on 87
482 capitol, industrial and polluted cities of the world. *Env. Sci. Eur.*, 33, 134,
483 <https://doi.org/10.1186/s12302-021-00575-y>.
484

485 Saharan, U. S., R. Kumar, P. Tripathy, M. Sateesh, J. Garg, S. K. Sharma, & T. K. Mandai
486 (2022). Drivers of air pollution variability during second wave of COVID-19 in Delhi, India,
487 *Urban Clim.*, 41, <https://doi.org/10.1016/j.uclim.2021.101059>.
488

489 Sicard, P., A. De Marco, E. Agathokleous, Z. Feng, X. Xu, E. Paoletti, J. Jaime, D. Rodriguez, &
490 V. Calatayud (2020). Amplified ozone pollution in cities during the COVID-19 lockdown, *Sci.*
491 *Tot. Env.*, 735, <https://doi.org/10.1016/j.scitotenv.2020.139542>.

492
493 Stavrakou, T., J.-F. Müller, M. Bauwens, T. Doumbia, N. Elguindi, S. Darras, C. Granier, D.
494 Smedt, C. Lerot, M. Van Roozendaal, B. Franco, L. Clarisse, C. Clerbaux, P. F. Coheur, Y. M.
495 Liu, T. Wang, X. Q. Shi, B. Gaubert, S. Tilmes, & G. Brasseur (2021). Atmospheric Impacts of
496 COVID-19 on NO_x and VOC Levels over China Based on TROPOMI and IASI Satellite Data
497 and Modeling, *Atmos.*, 12, <https://doi.org/10.3390/atmos12080946>.

498
499 Steinbrecht, W., Kubistin, D., Plass-Dülmer, C., Davies, J., Tarasick, D. W., von der Gathen, P.,
500 et al. (2021). COVID-19 crisis reduces free tropospheric ozone across the Northern Hemisphere.
501 *Geophys. Res. Lett.*, 48, e2020GL091987. <https://doi.org/10.1029/2020GL091987>.

502
503 Stone, K. A., S. Solomon, D. E. Kinnison, & M. J. Mills (2021). On recent large Antarctic ozone
504 holes and ozone recovery metrics, *Geophys. Res. Lett.*, 48, 22, e2021GL095232,
505 <https://doi.org/10.1029/2021GL095232>.

506
507 Torres, O., P. K. Bhartia, H. Jethva, & C. Ahn, Impact of the ozone monitoring instrument row
508 anomaly on the long-term record of aerosol products (2018). *Atmos. Meas. Tech.*, 11(5), 2701–
509 2715. <https://doi.org/10.5194/amt-11-2701-2018>.

510
511 Wargan, K., G. Labow, S. Frith, S. Pawson, N. Livesey, and G. Partyka (2017). Evaluation of the
512 Ozone Fields in NASA's MERRA-2 Reanalysis, *J. Climate*, 30, 2961–2988,
513 <https://doi.org/10.1175/JCLI-D-16-0699.1>

514
515 Yin, H., C. Liu, Q. Hu, T. Liu, S. Wang, M. Gao, S. Xu, C. Zhang, & W. Su (2021). Opposite
516 impact of emission reduction during the COVID-19 lockdown period on the surface
517 concentrations of PM_{2.5} and O₃ in Wuhan, China, *Env. Poll.*, 289, 117899,
518 <https://doi.org/10.1016/j.envpol.2021.117899>.

519

520 Ziemke, J. R., S. Chandra, B. N. Duncan, L. Froidevaux, P. K. Bhartia, P. F. Levelt, & J. W.
521 Waters (2006). Tropospheric ozone determined from Aura OMI and MLS: Evaluation of
522 measurements and comparison with the Global Modeling Initiative's Chemical Transport Model,
523 J. Geophys. Res., 111, D19303, doi:10.1029/2006JD007089.
524